Advancement in fruit drying through the analysis of moisture sorption isotherms: processing effects on Australian native fruits in comparison to apple

Paul Michalski[a], Md. Shahruk Nur-A-Tomal[a], Simon Crawford[b], Murray Rudman[c], Leonie van 't Hag[a,*]

[a] Department of Chemical and Biological Engineering, Monash University, Clayton, VIC, 3800, Australia

[b] Ramaciotti Centre for Cryo-EM, Monash University, Clayton, VIC, 3800, Australia

[c] Department of Mechanical and Aerospace Engineering, Monash University, Clayton, VIC, 3800, Australia

*Corresponding author. *E-mail address: leonie.vanthag@monash.edu*

Keywords

fruit, food drying, sustainable processing, moisture sorption, native foods, dynamic vapour sorption

Abstract

Australian native fruits are well-adapted to local climate and have growing interest in their nutritional and sensory qualities. Among the most highly produced are finger limes and muntries. However, published literature on their characterisation and especially their processing is limited. Water binding in foods is linked to their preservation through the amount of water microbes need to be active and the drying energy required. How processing affects this binding, however, is poorly understood. This work studied the water binding of apples compared with muntries and finger limes. Unlike in apple, water binding in native fruits was observed to increase after drying. This was correlated to increased breakdown of complex carbohydrates into simple sugars in native fruits. It is suggested this may be a feature of their drought adaptation. Together with a newly proposed equation for the drying heat required, these findings can guide more sustainable processing of Australian native fruits.

1. Introduction

Fruits and vegetables are essential components of human diets, particularly due to their high concentration of fibre and micronutrients. Their rapid spoilage and quality/nutritional degradation is largely the result of their high moisture contents. The varying structure and chemistry of dry matter in fruits determines their water binding capacity. Two foods of the same moisture content can have

substantial differences in the availability of that water for participation in degradation pathways, as quantified by the water activity (Jeantet, 2016). Water activity plays an important role in a food's shelf-stability, with correlations between the two being the subject of modelling. For example, Escobedo-Avellaneda et al. (2012) modelled the shelf-life of packaged vegetables dried to different extents. They found that knowing the water activities of these vegetables across a range of moisture contents, together with packaging permeation and area, could be used to predict how the probability of spoilage accumulated with time. The correlation between the water content and the water activity for a food as determined by measuring moisture sorption isotherms can therefore be used to engineer the processing conditions to improve shelf-life.

Isotherms for the sorption of water to the food matrix have for example been measured for apples, bananas, pineapples, grapes, apricots, tomatoes, carrots, potatoes, loquat, quince, and kiwifruit (Moraga et al., 2011, Kaymak-Ertekin and Gedik, 2004, Hossain et al., 2001, Kiranoudis et al., 1993, Moreira et al., 2008, Moraga et al., 2006). A number of different models have been proposed and tested as descriptors of these isotherms, including those suggested by Henderson, by Guggenheim, Anderson and de Boer (GAB), and by Brunauer, Emmett and Teller (BET) (Al-Muhtaseb et al., 2002). These have allowed for a more rigorous understanding of the interaction between foods and the water they contain. For example, fitting the GAB model to sorption isotherms of freeze-dried banana and apple at 20°C, Moraga et al. (2011) found a monolayer moisture content of 8.1% for the freeze-dried banana and 8.6% for the freeze-dried apple (see Section 3). This is representative of the 4-22% range typically reported for fruits and vegetables (Tsami et al., 1998, Kaymak-Ertekin and Gedik, 2004, Moraga et al., 2006, Kiranoudis et al., 1993, van 't Hag et al., 2020). Measurement and modelling of water sorption in a range of food materials has given insight into their water binding and shelf-stability.

Processing of fruits and vegetables affects water behaviour within them and therefore shelf-life. This phenomenon is not as well described, with most isotherms existing for the fresh or freeze-dried material only. However, in examples such as the work of Ben Haj Said et al. (2015) and van 't Hag et al. (2020), processing was shown to have significant effects on the water sorption in apples and African leafy vegetables. In the study of the effects that dehydration (via instant controlled pressured drop) as a pretreatment to freezing had on apple, Ben Haj Said et al. measured the sorption characteristics of this partially dried material before and after freezing. The consistent decrease measured in equilibrium moisture content post-freezing was correlated to the effect both drying and freezing had on apple drying and rehydration kinetics as well as changes in firmness. Pre-drying in this case was shown to eliminate the softening that freeze-thawing had on texture. In research on African leafy vegetables by van 't Hag et al., the effect of drying was investigated by measuring how sorption isotherms differed

before and after drying at 40°C. Here equilibrium moisture contents were lower across water activities for all samples measured after drying. This was correlated to drying-induced losses of cell structure observed using TEM. Correlating the changes in sorption isotherms with changes in micro- and nanostructure, texture, and rehydration ability allowed these researchers to better understand the changes that occurred during processing and so suggest best processing methods and conditions.

How food moisture sorption isotherms vary with temperature can elucidate the capacity and the energy of the binding between water and the food matrix. For example, the BET-defined monolayer moisture content, fitted to the sorption isotherms of grapes, apricots, apples, and potatoes, was shown to decrease with temperature between 30°C and 60°C (Kaymak-Ertekin and Gedik, 2004). The measurement of the temperature-dependence of sorption has also allowed the moisture content-dependent heat required to liberate water from its binding to the matrix to be determined. The net isosteric heat of sorption, or the heat required in excess of the latent heat of vaporisation to remove moisture from the food, was reported for dried raisins, figs, prunes, and apricots (Tsami et al., 1990). As moisture content decreased, the heat of sorption was observed to dramatically increase, which the authors attributed to the sorption of a monolayer being preferred at low moisture contents. The net isosteric heat of sorption and its dependence on moisture content was not observed to substantially differ between these fruits. A model was used to fit the heat of sorption that was obtained for these materials, but this was purely empirical.

Australian native fruits (ANFs) are among the tens of thousands of plant species unique to Australia and have a long history of appreciation by First Nations Australians. Their evolution in Australian climate and soil means they are inherently better adapted to these conditions than introduced crops, frequently displaying a reduced need for irrigation, pesticide and fertiliser use, as well as an increased tolerance to droughts, floods, and heatwaves (Orians and Milewski, 2007). These latter features particularly make them crops of interest for ensuring future food security as climate change raises temperatures and increases the threat of extreme weather events (Seneviratne et al., 2023). Finger limes and muntries are among the most highly produced ANF crops. In 2019/2020 they were produced at a rate of 103 and 3.4 tonnes/year respectively within Australia (Laurie, 2020). This industry is growing, with the farm gate market value projected to grow by 8.0% p.a. for finger limes and 2.8% p.a. for muntries between 2019/2020 and 2025. The market interest in ANFs is both within Australia as well as overseas. For example, as of 2021, 10 tonnes/year of finger lime are exported internationally, while global cultivation efforts have begun that include 12,000 trees in California and 100,000 trees in Guatemala (Glover et al., 2021). ANFs have also been shown to contain high amounts of protein and phenolic compounds (a class of antioxidants) compared to more commonly eaten fruits (Richmond et

al., 2019). However, nutritional and phytochemical characterisation of ANFs is still incomplete (Table 1), and where values are available the data is limited and often from one batch grown in one location.

Table 1: Selected data on previously reported nutritional data for ANFs where available (per 100 g w.b.). Data for apple is also presented for comparison (GAE: gallic acid equivalent, -: no published data found, G: glucose, S: sucrose, F: fructose, 1: (USDA, 2018), 2: (Netzel et al., 2007), 3: (Richmond et al., 2019), 4: (Francini and Sebastiani, 2013))

	Apple	Muntrie	Finger Lime
Protein (g)	0.26[1]	-	1.6[3]
Fat (g)	0.17[1]	-	1.0[3]
Carbohydrate (g)	13.8[1]	-	5[3]
Sugars (g)	2.43[G]/2.07[S]/5.9[F,1]	-	1.2[F+G,3]
Vitamin C (mg)	4.6[1]	16[2]	58.5[3]
Total Phenolics (mmol GAE)	0.070-3.442[4]	6.712[2]	8.65-10.93[2]
Energy (kJ)	218[1]	-	144-411[3]

While the industry of their cultivation and processing is growing, an understanding of how ANFs are affected by processing, specifically preservation, is absent from literature. For larger-scale process engineering of ANFs, a rigorous understanding of their processing-property relationships is needed. This would extend their shelf-lives and increase market penetration of ANFs while minimising quality loss and the cost and energy of processing. Through such an understanding of ANFs, the processing of more climate-tolerant crops in general, which may have different moisture sorption regulation properties, may be enabled to better protect future food security.

The research described in this work, therefore, characterises the moisture sorption phenomena in the ANFs muntries and finger limes as well as apples for comparison. This informs the minimum extent of drying that must be performed to achieve products with a range of water activities. How oven- and freeze-drying affected the sorption behaviour of these fruits, as well as qualities associated with water binding such as crystallinity, carbohydrate chemistry, and ultrastructure, were also examined. Changes in these latter properties were used to describe the processing-structure correlations that exist in apple, not previously reported in literature, as well as the measured ANFs. The measured sorption phenomena were modelled to describe facets of water binding dynamics. Based on these models a new analytical expression was derived that accurately approximates the energy requirements of drying. To the best of our knowledge, no analytical expression has been reported for the functional dependence of the net isosteric heat of sorption on moisture content for any food before. Such an expression has value in designing and optimising more bespoke dryers for the processing of ANFs as

well as other foods. These findings will inform the minimal but effective preservation of fruits and the minimum energy required to be able to do this for more sustainable processing.

2. Materials and Methods

2.1. Materials

Analytical grade petroleum ether, propylene oxide, magnesium chloride (99.99% purity), potassium chloride (99.8% purity), and lithium chloride (99.98% purity) were sourced from Merck Life Science (Bayswater, Victoria, Australia). A Megazymes K-SUFRG Sucrose/D-Glucose/D-Fructose enzymatic assay kit was obtained from Bio-Strategy (Campbelfield, Victoria, Australia), and 2,5-bis(5-tert-butyl-2-benzo-oxazol-2-yl) thiophene (BBOT) from Thermo-Fisher Scientific (Scoresby, Victoria, Australia). Pure (grade 4.2) compressed nitrogen was supplied by BOC (Dandenong South, Victoria, Australia) and Epon/Araldite resin by Electron Microscopy Sciences (Hatfield, Pennsylvania, USA). Glutaraldehyde (25%), paraformaldehyde (16%), uranyl acetate, lead citrate, potassium ferricyanide, sodium cacodylate trihydrate, and osmium tetroxide were sourced from ProSciTech (Kirwan, Queensland, Australia).

Muntries were donated by Ni Ni Well (Nhill, Victoria, Australia), finger limes (Rick's Red) were donated by OZ Finger Lime (Glenroy, Victoria, Australia), and apples (Pink Lady) were purchased from Monash Merchant (Clayton, Victoria, Australia). Whole fruits were air frozen at harvest (or after purchase in the case of apple) at -18°C using a SFT45-2 freezer (Skipio, Campbelfield, Victoria) until analysed or further processed. Freeze-drying of approximately 90 g of the frozen material was conducted at 0.04 mbar with an Alpha 1-2 LD-Plus freeze-dryer (John Morris, Victoria, Australia) until sample masses changed by < 0.1 g/h. Oven-drying of the frozen material was conducted with a Memmert UF55 oven (John Morris, Victoria, Australia). Approximately 90 g of fruit was dried at both 40°C and 60°C at 20% fan speed and 50% vent opening until sample mass changed by < 0.1 g/h. Dried samples were homogenised with a coffee grinder. They were then sealed using a FoodSaver® GameSaver™ VS9000 vacuum sealer (Sunbeam, NSW, Australia) in plastic vac-seal FoodSaver® pouches (Sunbeam, NSW, Australia) for dry storage until analysis.

2.2. Methods

2.2.1. Dynamic Vapour Sorption (DVS)

Sorption and desorption isotherms were obtained by using a DVS Adventure 1 (Surface Measurement Systems, London, UK). The instrument humidity control used an open control loop based on mass flow controller calibration using saturated salt slurries of KCl, LiCl, and $MgCl_2$. Of the dried, packaged, and

stored samples described in Section 2.1, 17 mg of sample was loaded via a steel pan into the instrument. The sample was allowed to equilibrate at 90% relative humidity, then 85%, 80%, 75%, 70%, and then in decreasing steps of 10% until 0%, at which point it remained at 0% for 600 minutes before increasing humidity in the reverse order. Equilibrium was considered reached once the sample mass changed by less than 0.0012%/min of its mass at the beginning of each humidity step. The humid atmosphere was generated through the supply of nitrogen and milliQ water to the instrument, and the humid gas flow over the sample was 200 sccm (except at 60°C, where the flow was 100 sccm). For dried samples, measurements were conducted two weeks after drying and dry storage at room temperature.

2.2.2. XRD

The samples were placed on a PMMA sample holder (C79298A3244D82, Bruker, USA) featuring a diameter of 51.5 mm and a height of 8.5 mm. X-ray diffraction patterns for the samples were obtained using a D8 ADVANCE (Bruker, USA), utilising Cu-Kα radiation at 40 kV and 40 mA. These patterns were recorded over a 2θ range of 5° to 80°, with a step size of 0.010° and a step time of 144.0 s. The DIFFRAC.EVA software package was used to determine the crystallinity and amorphous content of the samples. First, the background of the patterns was set manually. Then, 'Compute Crystallinity' was selected from the 'Crystallinity' tab, which provided values for Global Area and Reduced Area based on the broad amorphous peak area.

2.2.3. TEM

Pieces of fruit tissue, approximately 1 mm^3 in size, were placed into primary fixative for 24 hours at room temperature. The fixative consisted of 2.5% glutaraldehyde and 2% paraformaldehyde in 0.1 M sodium cacodylate buffer. The tissues were then rinsed twice in buffer for 1 hour. Secondary fixation was performed using 1% osmium tetroxide and 1.5% potassium ferricyanide in cacodylate buffer for 2 hours at room temperature. The tissues were rinsed in three washes of milliQ water for 10 minutes each and finally overnight in milliQ water.

The fixed tissues were dehydrated by incubating in increasing concentrations of ethanol for 24 hours at each step, consisting of 30, 50, 70, 90 and 100% ethanol. Dehydrated tissues were incubated for 1 hour in 100% propylene oxide. Tissues were then incubated in a mixture of Epon resin and propylene oxide at a ratio of 1:1 and ‘biowaving’ in a PELCO BioWave® Pro (Ted Pella Inc., California, USA) for 3 minutes at 250 W, followed by incubation for 24 hours at room temperature. This process of ‘biowaving’ and incubating for 24 hours was repeated with a 2:1 Epon/ethanol mixture and two steps

of 100% freshly made epon resin. Following the embedding steps the tissue samples were placed into BEEM capsules with fresh resin and polymerised for 48 hours in an oven at 60°C.

Resin embedded tissue was sectioned with a Diatome diamond knife using a Leica UCS ultramicrotome. Sections of thickness 80 - 90 nm were collected onto 150 mesh copper/palladium grids and stained sequentially with 1% uranyl acetate for 10 minutes and lead citrate for 5 minutes. The sections were imaged in a JEOL 1400+ transmission electron microscope (JEOL Ltd., Japan) at 80 kV, and images of cells captured with a digital camera at a resolution of 2K x 2K.

2.2.4. Macronutritional Profile

Freeze-dried samples were used for macronutrient characterisation. Moisture content was determined in triplicate at 130°C using an MB25 moisture analyser (Ohaus, Victoria, Australia). Four replicates of the protein content were measured through the CHNS combustion method, finding the nitrogen content using a FlashSmart elemental analyser (Thermo-Fisher Scientific, Victoria, Australia) and BBOT standards. A Kjeldahl factor of 5.36 was used to convert nitrogen content to protein content. This was based on the work of Salo-väänänen and Koivistoinen (1996) which found more specific Kjeldahl factors for different food groups as opposed to the value of 6.25 often used for food in general.

The standard AOAC method 2003.06 (AOAC, 2005) was the basis for the ash content measurements (done in duplicate). Pre-weighed porcelain crucibles were loaded with samples and weighed before being placed in a CF1200-4.5L muffle furnace (Across International, Victoria, Australia). Here the sample crucibles were heated at 100°C for an hour before being heated at 525°C for 18 hours to dry ash. After cooling, samples were inspected for evidence of charring. If present, a few drops of milliQ water were added to the crucible before repeating the heating sequence until a pale grey fine ash remained and could be weighed.

For the fat content, 4 g of sample was weighed into a cellulose thimble and subsequently placed in a Soxhlet apparatus. Here 200 mL of petroleum ether was used to extract crude fat from the sample over the course of 16 hours. The solvent was first evaporated from the extraction flask using a Rotavapor R-210 rotary evaporator (In Vitro Technologies, Victoria, Australia) at 60°C and 580 mbar for 15 minutes. Residual solvent was then further dried in a 27G SEM drying oven (Labquip™, Victoria, Australia) at 60°C until a consistent weight was measured. Fat contents were measured in duplicate.

Carbohydrate content was calculated by difference, i.e. the sample mass after subtraction of moisture, protein, fat, and ash content. Energy content was calculated using the specific Atwater factors for fruit of 14.1 kJ/g protein, 35 kJ/g fat, and 15.1 kJ/g carbohydrates (Merrill, 1973).

2.2.5. Sugar Contents

Sugar assays were performed on frozen samples (homogenised immediately prior to analysis) and samples that had been oven-dried, each in triplicate. Samples were each added to 400 mL milliQ water before being sonicated for 30 minutes in a Sonorex RK255/H/CH ultrasonic bath (John Morris, Victoria, Australia). They then underwent syringe filtration using 0.45 µm Supor® membranes in 25 mm Acrodisc® filters (Pall Corporation, New York, USA) and dilution in milliQ water by a factor of 3. These solutions were then assayed according to the Megazymes K-SUFRG Sucrose/D-Glucose/D-Fructose protocol. A Multipette® M4 - Multi-Dispenser pipette (Eppendorf, NSW, Australia) was used for the dispensation of solutions for the assay. The assays were performed in 10 x 10 x 45 mm polystyrene cuvettes (Sarstedt, Nümbrecht, Germany) and absorbances were measured at 340 nm using a Cary 60 UV-Vis Spectrophotometer (Agilent, Victoria, Australia).

3. Theory/Calculation

3.1. Moisture Sorption Isotherms

A number of models have been used in describing water sorption phenomena in foods. Ten common models were selected as candidates for modelling ANF sorption. These were the Oswin, Brunauer-Emmett-Teller (BET), Guggenheim-Anderson-de Boer (GAB), Halsey, Chen, Chung-Pfost, Henderson, Caurie, Sips, and Iglesias-Chirife models (Kaymak-Ertekin and Gedik, 2004, van 't Hag et al., 2020). Empirical, semi-empirical, and analytical models are included in this selection, and their definitions are included in the Supplementary Information Appendix 2 **Error! Reference source not found.**.

The Oswin, Henderson, Chen, Chung-Pfost and Iglesias-Chirife models are empirical, with Iglesias-Chirife also including a term $M_{0.5}$ for the moisture content at a water activity of 0.5 (Al-Muhtaseb et al., 2002, Chung and Pfost, 1967, Iglesias and Chirife, 1978). The Sips model expresses heterogeneous sorption with its constants K_S, N, and C describing the capacity, intensity, and energy of sorption respectively. In contrast, the Halsey model describes sorption of multilayers spanning a larger distance from the surface, with k being an empirical constant and n quantifying the decay in potential binding energy as distance is increased. The BET and Caurie models also depict sorption as occurring in layers, with a monolayer moisture content M_0 and a constant C related to the heat of sorption. The GAB model describes sorption as the binding of a monolayer of the water adsorbate to the food surface, as well as the binding of multilayers of adsorbate on top of this monolayer. These multilayers are energetically distinct from the monolayer but themselves undifferentiated. Because the GAB model was found to best fit the data in this work (see Section **Error! Reference source not found.**) it was used for the

241 derivation of an analytical expression of the net isosteric heat of sorption as outlined in Section 3.2.
242 The GAB model is expressed in Eq. (1).

$$M = \frac{M_0 K C a_w}{(1 - K a_w)(1 + (C - 1) K a_w)} \quad (1)$$

243 Eq. (1) gives a functional relationship between the water activity a_w and the moisture content (on a
244 dry basis) M. The model includes the parameters M_0 (the monolayer moisture content), K (a
245 thermodynamic quantity associated with multilayer sorption), and C (a thermodynamic quantity
246 associated with monolayer sorption). The latter two parameters are also described by the model as
247 having an Arrhenius-type temperature dependence in Eq. (2-3). Here, H_l is the enthalpy of the bulk
248 adsorbate material, H_m is the enthalpy of the adsorbate in the monolayer, and H_n is the enthalpy of the
249 adsorbate in the multilayers. Here and throughout this work, R and T are the universal gas constant
250 and the absolute temperature. The pre-exponential factors K_0 and C_0 are temperature-independent
251 entropic parameters associated again with the thermodynamics of multi- and monolayer sorption
252 respectively.

$$K = K_0 e^{\frac{H_l - H_n}{RT}} \quad (2)$$

$$C = C_0 e^{\frac{H_n - H_m}{RT}} \quad (3)$$

253 3.2. Net Isosteric Heat of Sorption

254 If the bulk adsorbate material behaves as an ideal gas under the measurement conditions, the
255 temperature-dependence of its latent heat of vaporisation is considered negligible, and its specific
256 volume when adsorbed is insignificant compared to its bulk specific volume, the Clausius-Clapeyron
257 equation can be expressed in terms of the net isosteric heat of sorption (q_{st}) as Eq. (4).

$$q_{st}(M) = R \left(\frac{\partial \ln(a_w)}{\partial \left(\frac{1}{T}\right)} \right)_M = Q_{st}(M) - \Delta H_v \quad (4)$$

In Eq. (4) Q_{st} is the isosteric heat of sorption and ΔH_v is the latent heat of vaporisation of the adsorbate material. Thus, q_{st} is a measure of the energy required in excess of the latent heat of vaporisation to liberate a unit amount of adsorbate to the bulk phase at a given moisture content.

Limited empirical approaches and no analytical approaches have been reported to model the functional dependence of q_{st} on the moisture content. Since the GAB isotherm model is analytical and best fit the measured isotherms (Section **Error! Reference source not found.**), it was used to derive an analytical expression for q_{st}. Expressing the GAB model in terms of M yields Eq. (5).

$$a_w = \frac{\zeta + \sqrt{\zeta^2 - 4M^2(1-C)}}{2MK(C-1)} \tag{5}$$

Where

$$\zeta \equiv M(C-2) - M_0 C$$

Solving Eq. (4) using Eq. (5) yields, after simplification (see Supplementary Information Appendix 3 for detailed derivation) Eq. (6).

$$q_{st}(M) = R\frac{\left(\Psi + \frac{\zeta\Psi + 2M^2\frac{H_n - H_m}{R}}{\sqrt{\zeta^2 - 4M^2(1-C)}}\right)C(C-1) - \left(\frac{H_l - H_n}{R}(C-1) + \frac{H_n - H_m}{R}C\right)\left(\zeta + \sqrt{\zeta^2 - 4M^2(1-C)}\right)}{\left(\zeta + \sqrt{\zeta^2 - 4M^2(1-C)}\right)(C-1)} \tag{6}$$

Where

$$\Psi \equiv M\frac{H_n - H_m}{R} - \frac{dM_0}{d\left(\frac{1}{T}\right)} - M_0\frac{H_n - H_m}{R}$$

Eq. (6) is an analytical model for the net isosteric heat of sorption with only five fitting parameters based on the sorption mechanisms described by the GAB model. It is expressed as a function of the moisture content and parametrised by the material-specific values of H_m, H_n, M_0 (and its derivative with respect to reciprocal temperature), and C. The parameter K is notably absent from the expression. The material-specific parameter associated with the entropy of multilayer sorption, K_0, does not affect the net isosteric heat of sorption; the only influence of multilayer sorption is through the multilayer enthalpy H_n. The parameter C is assumed to follow an Arrhenius-type temperature dependence as described by Eq. (3). However, since the net isosteric heat of sorption is only weakly temperature-dependent at these scales, C represents a temperature-independent limit for the temperatures

considered. The value of M_0 as obtained by the fitting of Eq. (6) is taken as a temperature-independent limit for the same reason, however it is not assumed to follow an Arrhenius-type relationship.

3.3. Statistical Analysis

Analysis was performed in MATLAB R2022a and used Eq. (7) and (8) for the goodness of fit (v being the number of degrees of freedom), including the sum of square errors (SSE). For access to the MATLAB scripts written for this analysis, see Appendix 2.

$$SSE = \sum \left(y_i^{measured} - y_i^{predicted}\right)^2 \tag{7}$$

$$\chi_v^2 = \sum \frac{\left(y_i^{measured} - y_i^{predicted}\right)^2}{v\left|y_i^{predicted}\right|} \tag{8}$$

Goodness of fit statistics are given for fits of the moisture sorption isotherms and net isosteric heats of sorption (

Table 2 and Supplementary Information Appendix 2 **Error! Reference source not found.**S1 and S2). Differences in protein values between fruits were analysed by a one-way ANOVA. The differences in sugar contents between fruits and the differences before and after drying were analysed by a two-way ANOVA followed by Tukey *post hoc* comparisons of the significantly different results.

4. Results and Discussion

The moisture sorption results of the DVS measurements are presented below, proceeded by the fitting of the net isosteric heat of sorption derived from these measurements. Following this, the changes in carbohydrate structure as measured by XRD and the changes in cellular structure as measured by TEM are given. The macronutritional profiles and the changes to sugar composition are then described. Finally, the changes to carbohydrate structure, cellular structure, and sugar composition are then compared to the differences in the moisture sorption behaviour.

4.1. Moisture Sorption Isotherms

Moisture sorption isotherms as measured with DVS describe the binding of water to the food material and relate how shelf-stability varies with moisture content. The changes in sample mass (and therefore

298 moisture content) were measured in response to changes in surrounding humidity. The relationship
299 between equilibrium moisture content and water activity for each measurement temperature formed
300 the moisture sorption isotherms. Isotherms measured at 25°C and 60°C for frozen and oven-dried (at
301 60°C) fruit samples are shown in Figure 1(a-c). Apples, muntries and finger limes all exhibited
302 significant increases in moisture content at high water activity, and relatively little change in moisture
303 content at lower water activity.

304 The shape and values taken by the isotherms are related to the class of food and its shelf-stability. The
305 observed isotherm shape is that of type-III isotherms, characteristic of high-sugar foods as previously
306 reported (Al-Muhtaseb et al., 2002, Rao et al., 2005). With minimal pathogenic proliferation at water
307 activities below 0.6, the moisture content to which this water activity corresponds is considered the
308 maximum microbially safe moisture content. From the desorption of frozen fruit (25°C isotherms), the
309 microbially safe moisture contents can be reported as 14% d.b. for finger lime, 8.0% for muntrie, and
310 15% for apple. In comparison, equivalent microbially safe moisture contents (interpolating water
311 activities and approximating with 30°C isotherms) measured by Kaymak-Ertekin and Gedik (2004) were
312 30% for grapes and 36% for apples. The moisture content measured in this work was lower in
313 comparison. In the work of Kaymak-Ertekin and Gedik (2004), however, the apple was frozen, and
314 freezing is seen to reduce the sorption that occurred in ANFs compared to select isotherms of fresh
315 fruit in Appendix 1 Figure S1. This is suggested to be the reason for the difference in microbially safe
316 moisture content of apple. This is also consistent with the effect of freezing on sorption described in
317 the work of Ben Haj Said et al. (2015) in Section 1.

318 Isotherms at 25°C showed that oven-drying (at 60°C) frozen fruit consistently reduced the equilibrium
319 moisture content for all water activities. In contrast, isotherms measured at 60°C showed that, for
320 muntrie and finger lime, oven-drying (at 60°C) increased the equilibrium moisture contents for all
321 water activities compared to the frozen sample. This was the opposite for apple, where oven-drying
322 (at 60°C) reduced moisture sorption.

323 The effect was investigated further for 40°C isotherms and included muntries that had been oven-dried
324 (at 40°C) and freeze-dried (Figure 1(d)). At this measurement temperature, freeze-dried muntries
325 bound more water than the oven-dried (at 40°C), which in turn bound more water than the frozen
326 muntries at all water activities. The oven-dried (at 60°C) muntries bound the most water for water
327 activities greater than 0.75 among the 40°C isotherms. It was also this water activity window of 0.60 -
328 0.75 in which the effects of isotherm measurement temperature changed; below this water activity,
329 sorption uniformly increased with temperature, but for greater water activities the 40°C isotherms

showed greater equilibrium moisture contents. All drying processes increased the equilibrium moisture content achieved at all measured water activities when measuring at 40°C. Additional isotherms generated are included in Supplementary Information Appendix 1 Figure S1.

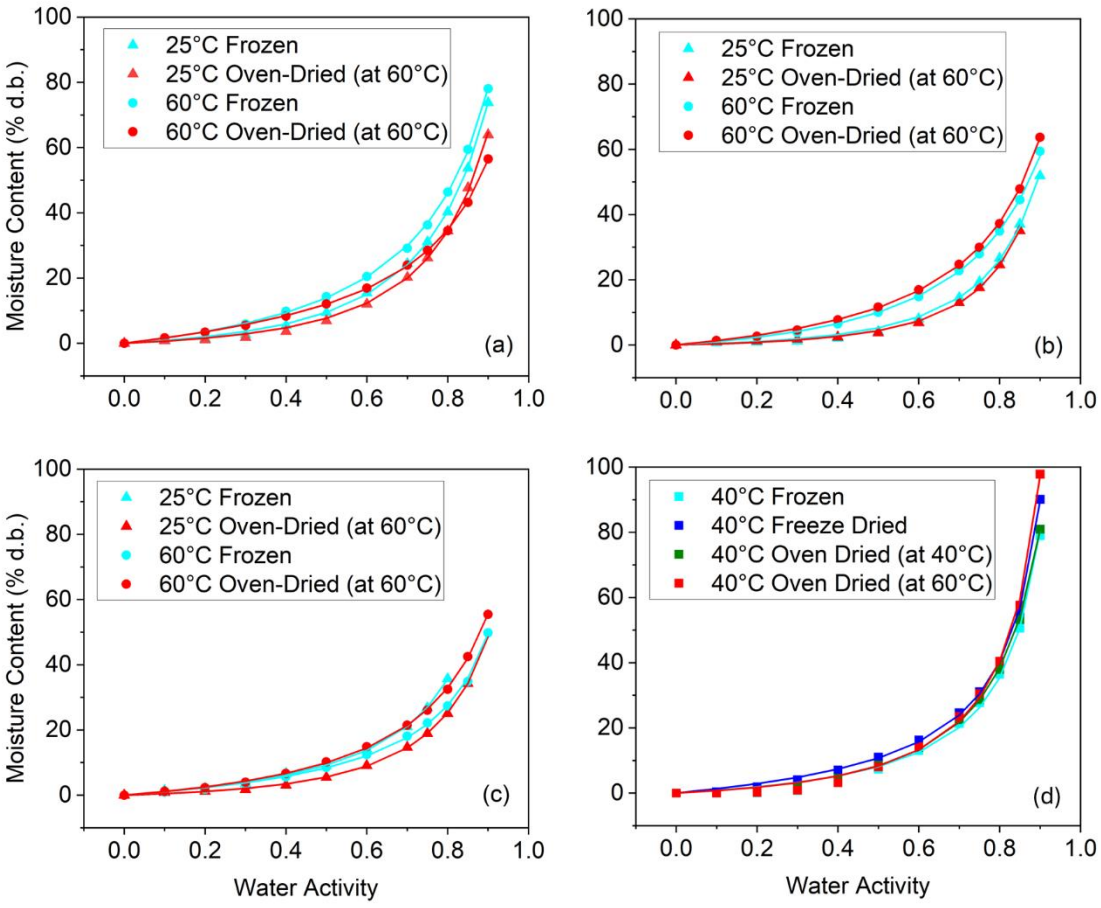

Figure 1: Select desorption isotherms (and best GAB fits) measured at 25°C and 60°C of frozen and oven-dried (dried at 60°C): (a) apple; (b) muntrie; (c) finger lime, as well as the 40°C isotherms describing the sorption of frozen muntries (d) after a range of processing conditions: data (▪) and GAB fit (–)

The increases in sorption observed in ANFs is contrary to what was measured for African leafy vegetables (van 't Hag et al., 2020), where sorption uniformly decreased after drying. It is also contrary to the wider observations of the irreversible changes fruits undergo during drying. These changes do not allow rehydration to the same extent as they could before drying when equilibrated to the same water activity (Ben Haj Said et al., 2015), let alone accumulate a greater moisture content. In this regards muntries and finger lime display distinctly different sorption behaviour.

The performance of the models used to describe the sorption behaviour of these samples and the parameter values corresponding to their best fits are indicated in Supplementary Information

(Appendix 2 **Error! Reference source not found.**) for the 60°C isotherm of frozen muntries as a representative example. Since the GAB model was consistently the isotherm model that minimised the *SSE*, it was selected as the most accurate representation of the sorption mechanism in these systems. This being the case for individual isotherms, isotherms for each sample were then fitted again. This time the isotherms corresponding to a sample across the measured temperatures were fitted simultaneously to also fit the Arrhenius-type temperature dependence of the model's parameters (Appendix 2 **Error! Reference source not found.**). By this latter fitting, M_0 (which was allowed to vary with temperature) was found to take values between 7.1% d.b. in the case of frozen muntries at 25°C and 25% in the case of oven-dried muntries at 60°C. These GAB monolayer moisture contents were consistent with the ranges reported for other, relatively sugar-rich fruits and vegetables as described in Section 1. To extend this model and improve the goodness of fit, however, the net isosteric heat of sorption was modelled and presented in Section 4.2.

4.2. Net Isosteric Heat of Sorption

To transform the isotherm data collected into measured values of the net isosteric heat of sorption, isosteres (curves following the relationship between a_w and T at constant M) were constructed for muntries and finger limes using the moisture contents of the 40°C isotherms and interpolating the 25°C and 60°C isotherms to obtain the values of a_w at those moisture contents. For apple – without data taken at 40°C – the moisture contents of the 25°C isotherms were used and the 60°C isotherms were interpolated to find the values of a_w at those moisture contents. Transforming this data to show how $ln(a_w)$ varies with $1/T$, and assuming a negligible temperature-dependence of the net isosteric heat of sorption, the gradient of the linear fit to each of these isosteres yields q_{st} for that value of M.

The net isosteric heat of sorption was then derived through the transformation of the isotherm data as outlined in Section 3.2. The transformed data was then used to validate whether the newly proposed model for q_{st} provided in Eq. (6) was valid. These experimentally derived values for $q_{st}(M)$, as well as the best fit of the model described in Eq. (6) to these data, are shown in Figure 2.

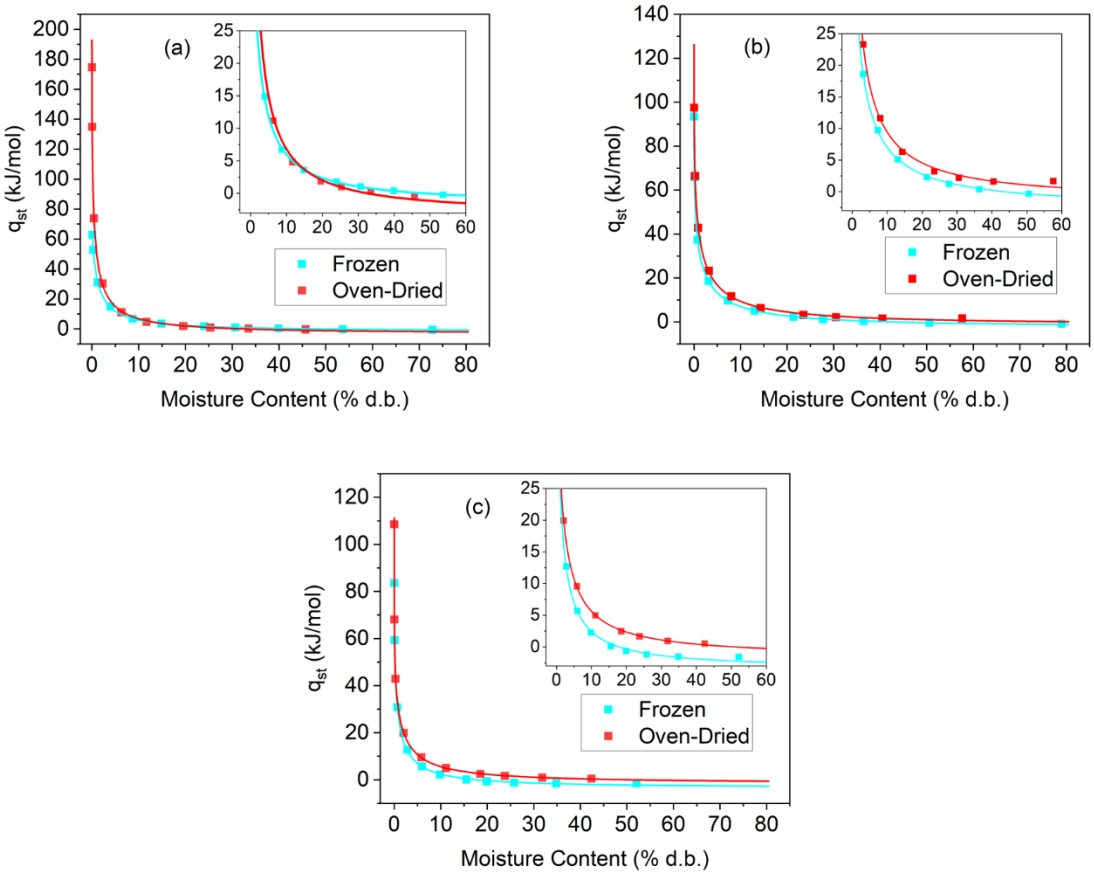

Figure 2: Net isosteric heat of sorption data (▪) and fitted models (–) of frozen and oven-dried (dried at 60°C): (a) apple; (b) muntrie; (c) finger lime. Inserts show moisture contents of 0 to 60% d.b in the region of 0 to 25 kJ/mol to clarify differences and demonstrate the goodness of fit.

The values of q_{st} were highest as moisture contents approached zero, sharply decreasing as moisture content increased. The functional shape exhibited by $q_{st}(M)$ is as expected for a high-moisture food. As described in Section 1, the amount of energy required to liberate water increases significantly as more water is removed (Tsami, 1991). This trend as well as the range of values adopted was consistent with those reported by Kaymak-Ertekin and Gedik (2004) for apple. The smoother curve of this new data is hypothesised to be due to the increased precision afforded by DVS compared to the static-gravimetric method. Compared to those reported by Kaymak-Ertekin and Gedik (2004), the generally reduced values of q_{st} here measured for apple are thought to be due to the effect of freezing in this study, which as identified in Ben Haj Said et al. (2015), can cause reduced sorption. To verify this, select isotherms of fresh ANF samples were also measured and supported the reduced sorption that occurs with freezing (Appendix 1 Figure S1). Bulk water with minimal binding is removed preferentially, then water in progressively more active sites is removed, requiring greater energy. Figure 2(b-c) shows that oven-drying affects muntries and finger limes in such a way as to increase the energy required for

moisture to escape at all moisture contents. For apple, on the other hand, this trend holds only where $M < 0.15$, above which the trend reverses (Figure 2(a)). This is consistent with the isotherm results that show increased water binding after drying in the case of the ANFs and not in the case of apple. This phenomenon has not previously been reported for either conventional or native fruits. It is suggested that the difference in this binding energy trend is associated with the increased water binding observed in the isotherms of dried ANFs compared to frozen.

Fitting of the q_{st} data to the GAB-derived model (Eq. (6)) exhibits close agreement, quantified by the *SSE* values listed in

Table 2. The values obtained for *C* varied between 0.17 for oven-dried finger lime and 0.32 for oven-dried apple. This range is consistent with the values for *C* obtained in literature by isotherm modelling, e.g. the range of 0.42 - 1.54 obtained for sultanas by Maroulis et al. (1988). In muntries and finger limes, the difference between the multilayer and bulk water enthalpy was decreased from 2.71 to 1.58 and from 3.55 to 1.68 kJ/mol respectively by drying. In apple, drying increased this difference from 1.78 to 3.40 kJ/mol. These enthalpy differences were similar in range to those determined from the sorption isotherms of fresh apples (0.48 kJ/mol) and potatoes (3.49 kJ/mol) by Kaymak-Ertekin and Gedik (2004). While drying raised the multilayer enthalpy in the ANFs, the enthalpy difference between the mono- and multilayer increased more substantially with drying, from 298 to 359 kJ/mol in muntries and from 288 to 487 kJ/mol in finger lime. Once again following an opposite trend, the corresponding change to the same enthalpy difference in apple decreased from 586 to 452 kJ/mol. Thus, while drying muntries and finger limes raises the enthalpy of the multilayer to be closer to that of liquid water and decreases the enthalpy of the monolayer, the opposite occurs as apples are dried. These enthalpy differences were an order of magnitude greater than the range of values typically determined through isotherm modelling. For example, 23.4 kJ/mol was the average value for this difference in enthalpy determined by Maroulis et al. (1988) for dried figs, prunes, apricots, and raisins. Also, the monolayer moisture content was determined to have values between 0.14% and 0.31% d.b., approximately 2 orders of magnitude less than the monolayer moisture content range literature provides for GAB fits to the isotherms as discussed in Sections 1 and 4.1. These differences may arise from the combination of data at all temperatures to express a temperature-independent net isosteric heat of sorption. For instance, the rate of change of monolayer moisture content with respect to reciprocal temperature was determined to be about -100 K, i.e. the monolayer moisture content strongly increases with temperature. The single value of M_0 determined here may then be a low-temperature limit to the monolayer moisture content. More generally, it is suggested the differences in values obtained by

fitting the isotherms directly versus fitting the net isosteric heat of sorption come from the temperature-independence of the latter.

Table 2: Values of net isosteric heat of sorption fitting parameters based on the sorption isotherms of frozen and oven-dried (at 60°C) apple, muntrie, and finger lime. Variation in fitting parameters is based on 68% confidence intervals. Extreme values which change the sign of the parameter are not considered physically meaningful.

	Apple		Muntrie		Finger Lime	
	Frozen	Oven-Dried	Frozen	Oven-Dried	Frozen	Oven-Dried
C (-)	0.2335 ± 1.813	0.3155 ± 0.0192	0.2451 ± 0.0086	0.2557 ± 0.0992	0.2633 ± 0.0451	0.1661 ± 0.0026
M_0 (% d.b.)	0.138 ± 1.21	0.177 ± 0.033	0.309 ± 0.032	0.285 ± 0.180	0.175 ± 0.055	0.148 ± 0.008
H_n -H_m (kJ/mol)	585.5 ± 5841	451.9 ± 74.23	298.1 ± 24.63	359.0 ± 251.35	288.3 ± 102.3	487.4 ± 15.311
H_l -H_n (kJ/mol)	1.784 ± 0.155	3.399 ± 0.4818	2.714 ± 0.1684	1.581 ± 0.55	3.546 ± 0.3128	1.677 ± 0.1239
$dM_0/d(1/T)$ (10^3 K)	-0.1078 ± 0.0043	-0.1389 ± 0.0084	-0.1521 ± 0.0055	-0.1676 ± 0.0173	-0.0833 ± 0.0065	-0.1078 ± 0.0027
SSE	0.2754	2.0682	0.2512	1.6421	0.9643	0.0989
χ_v^2	0.0066	0.3827	0.0424	0.1436	0.2618	0.0174

The goodness of fit for this proposed model, as quantified by χ_v^2, takes into account the differences in both the degrees of freedom and the quantity being measured between these fits and those of **Error! Reference source not found.**. This goodness of fit is better in the global fitting of the net isosteric heat of sorption than in the global fitting of the GAB isotherms at multiple temperatures for the majority of samples. One fewer parameter is also required with this approach due to the absence of a K term. Therefore, while the fitting to the net isosteric heat of sorption places additional assumptions as outlined above, the values of

Table 2 (from the net isosteric heat of sorption) are those accepted here. The performance of this model supports the validity of the GAB model description of sorption, and with its validity thus supported this approach offers a new tool for food process engineering. The net isosteric heat of sorption q_{st} can be understood to be a differential quantity of heat required to liberate a differential quantity of water, changing the moisture content only infinitesimally. It is proposed then that the total heat per unit mass (dry basis) required to dry a food from an initial moisture content M_i to a desired

final moisture content of M_f (which can be chosen using the sorption isotherms together with a choice of a_w and therefore shelf-life) can be predicted using Eq. (9).

$$Q|_{M_i}^{M_f} = \frac{1}{MW}\left(\Delta H_v - \int_{M_i}^{M_f} q_{st}(M)dM\right) \quad (9)$$

Here q_{st} is expressed as in Eq. (6) and MW is the molecular weight of water.

4.3. XRD

XRD provides information on sample structure by measuring the intensity and scattering angle of X-rays incident on the sample. It was performed in this study to assess changes in carbohydrate structure following processing. Performing XRD on apples, muntries, and finger limes produced the diffractograms in Figure 3. Freeze-dried (not frozen) samples are used as a benchmark in these XRD results to compare with oven-dried samples. Freeze-drying introduces minimal physicochemical changes compared to oven-drying, and low-moisture samples were required with this instrument setup. All three XRD diffractograms have broadly consistent diffuse peak contributions reaching maxima at 21.4° and 37.6°. The major exceptions to this are the sharp peaks at 21.5° and 23.8° in muntries. The areas under the curves were lower in the oven-dried samples compared to the freeze-dried: 8.9% lower for apple, 15.3% for muntrie, and 9.8% for finger lime. The diffuse peaks indicate the predominance of an amorphous structure. Possible origins for the diffuse signals at 21.5° and 23.8° are the starch and pectin components of the fruits respectively (Mutungi et al., 2012, Kazemi et al., 2023). The sharp signals in muntries are consistent with the presence of crystalline cellulose (Bezerra et al., 2014). Assuming structure at this scale is the same in the freeze-dried as in the frozen material, XRD reveals that oven-drying reduces the integrated intensity of the amorphous signal. This signal loss suggests that oven-drying reduced the amount of the complex polysaccharides present that contributed to the diffuse peaks, especially in muntries and finger limes (Appendix 5). This is consistent with how XRD diffractograms of amorphous gelatinised starch have been reported to have a reduced amorphous signal following hydrolysis (O'Brien and Wang, 2008) as well as following drying (Ye and Baik, 2024). It is suggested the processing-induced changes observed in carbohydrate chemistry and structure are correlated to the changes observed in water sorption (see Section 4.7).

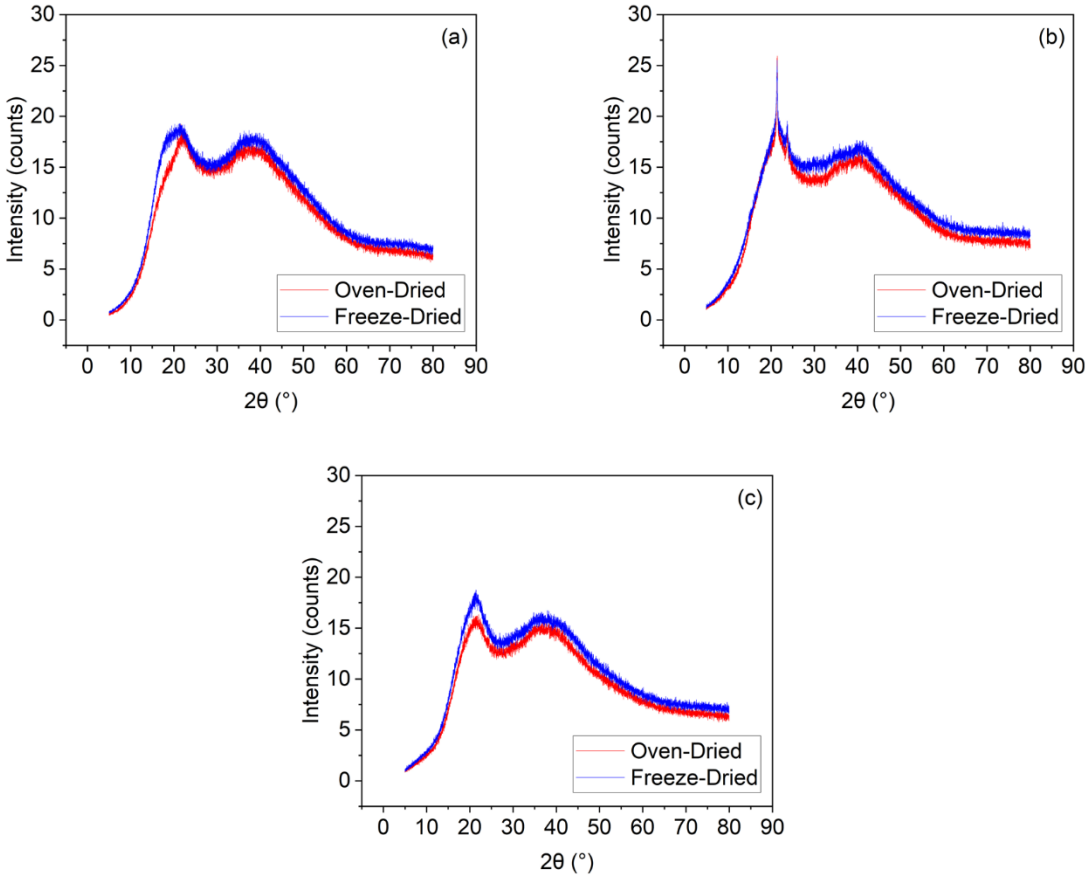

462

463 *Figure 3: XRD diffractograms of freeze- and oven-dried (at 60°C): (a) apple; (b) muntrie; (c) finger lime.*

464 ## 4.4. TEM

465 TEM can be used to image the micro- and nanostructure of a food material and indicate the changes
466 induced by processing. In this work, TEM was used to image the cellular features of apples, muntries,
467 and finger limes when fresh, frozen, and oven-dried (Figure 4). Representative TEM images were
468 selected for Figure 4, with select annotations describing proposed ultrastructural features.
469 Chloroplasts undergoing degradation of their thylakoid membranes into lipid bodies can be observed
470 in the fresh finger limes and muntries (Figure 4 (b, d)). Starch crystals are tentatively identified as
471 associated with the cell wall of a parenchymal cell in fresh finger lime (Figure 4 (c, g, k)). Finger limes
472 (in Figure 4 (c, d, g, h, k, l)) as an example of a hesperidium, contain juice vesicles (the edible portion
473 of the fruit) that are multicellular sacs. The structures identified in the finger limes are similar to those
474 that have been identified in fully ripe juice vesicles of grapefruit, another hesperidium (Burns et al.,
475 1992). The chloroplasts can also be observed breaking up and being exposed by the freezing and
476 especially the drying process in both the muntries and the finger limes (Figure 4 (b, j, d, h, l). As the
477 muntries were first frozen (Figure 4 (e, f)) and then dried (Figure 4 (i)), the cell membrane deformed

and separated as the cell wall loosened. This is similar to what has been observed occurring during ripening of Goji berry, where berry mesocarp was also studied (Zhang et al., 2024). In studying Goji berry ripening, Zhang et al. (2024) linked this phenomenon to the depolymerisation of cell wall polysaccharides by enzymes associated with ripening. The micrographs indicate processing-induced changes to the fruit cellular features consistent with the opening up of these features and the depolymerisation of their carbohydrate components. The correlation of this to changes in water binding are further discussed in Section 4.7.

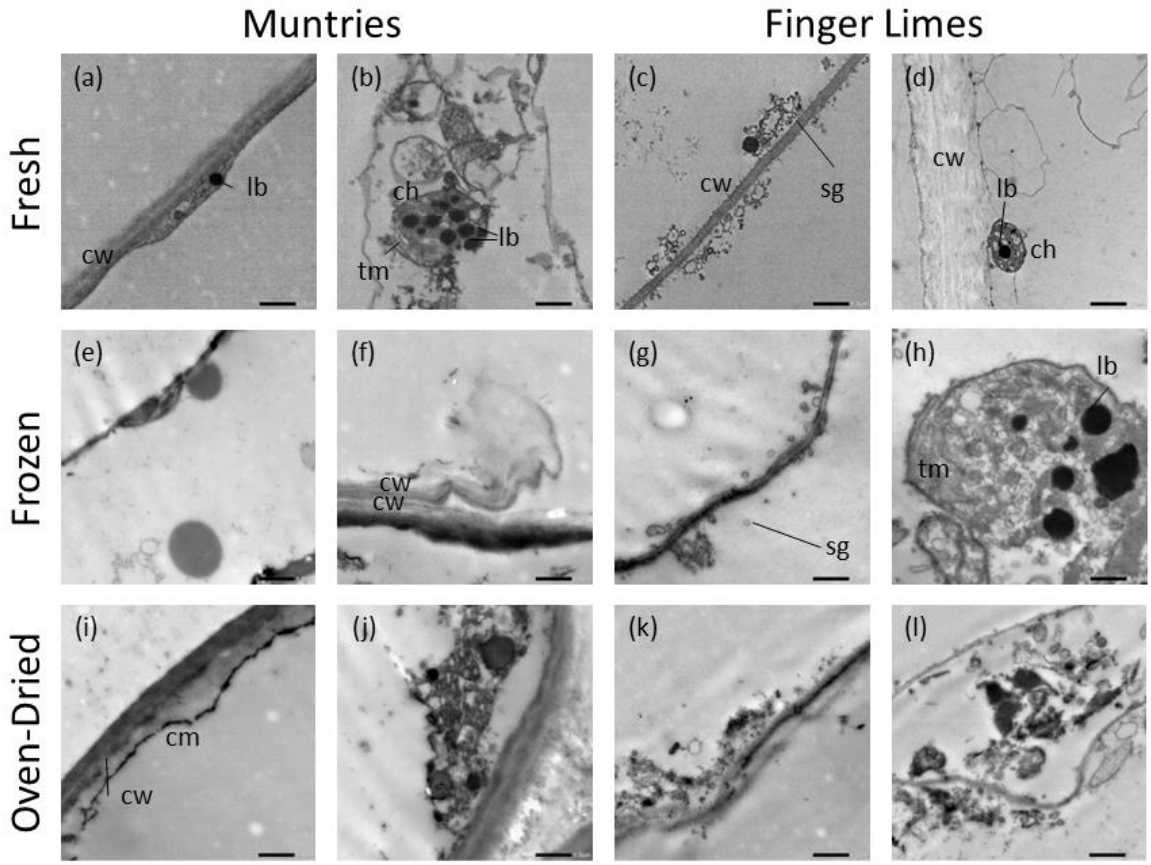

Figure 4: TEM micrographs of fresh, frozen, and oven-dried (at 60°C) muntries and finger limes. Scale bar represents 1.0 µm. cw - cell wall; sg - starch granules; cm – cell membrane; ch - chloroplast; tm – thylakoid membrane; lb – lipid bodies.

4.5. Macronutritional Content

Characterising the macronutrient composition of ANFs is necessary for understanding their nutritional and health applications but can also give insight into their physicochemical properties. The carbohydrate and energy content of apples and muntries were similar, varying from 15-18 g/100 g w.b.

and 238-299 kJ/100 g respectively, with muntries having the greater carbohydrate content and therefore energy content. Finger limes were not as rich in carbohydrates or energy, however, with 13 g/100 g w.b. and 177 kJ/100 g respectively. On a dry basis the fruits were all between 87.1 and 97.5% carbohydrate. Of the macronutrients, statistical testing was conducted on the protein contents. One-way ANOVA and Tukey tests demonstrated the protein contents of the ANFs (0.99 g/100 g w.b. for muntries and 0.83 g/100 g for finger limes) were significantly ($p < 0.05$) greater than for apple (0.13 g/100 g). Apples and finger limes were measured as having similar moisture contents (84.1 and 84.2 g/100 g w.b. respectively) while muntries were relatively low in moisture (79.7 g/100 g). The ANFs were measured as being higher in fat than apple (0.27 - 0.63 g/100 g vs. 0.08 g/100 g) as well as higher in ash (0.79 - 0.57 g/100 g vs. 0.19 g/100 g). The macronutrient contents measured for apples are broadly consistent with reference values from the USDA (see Table 1).

Table 3: Macronutritional profiles of apple, muntrie, and finger lime (per 100 g w.b.). Values attached to different letters are statistically significant to each other ($p < 0.05$).

	Apple	Muntrie	Finger Lime
Moisture (g)	84.14 ± 1.91	79.70 ± 1.73	84.23 ± 3.58
Protein (g)	0.1267 ± 0.0101[a]	0.9946 ± 0.0389[b]	0.8272 ± 0.1784[b]
Fat (g)	0.078 ± 0.10	0.27 ± 0.07	0.63 ± 0.52
Ash (g)	0.1934 ± 0.0079	0.7859 ± 0.0201	0.5739 ± 0.0374
Carbohydrate (g)	15.46 ± 0.37	18.24 ± 0.40	13.74 ± 0.80
Energy (kJ)	238.0 ± 0.4	299.0 ± 0.4	176.6 ± 1.0

4.6. Sugar Contents

Because of their prevalence in fruit, their nutritional relevance, and the strong influence of sugars on water-binding in food (Rao et al., 2005), fructose, glucose, and sucrose were also measured via enzymatic assay (Table 4). Two-way ANOVA was used to assess statistical significance of samples measured in triplicate. Among the undried (frozen) fruit, sucrose, glucose, and fructose were all highest in apple. Glucose and fructose were significantly ($p < 0.05$) greater in apple than in muntrie, itself significantly greater than in finger lime. Sucrose was also significantly greater in apple than in muntrie. Since muntries contained more total carbohydrates than apple while apple contained more of the sugars measured, it is suggested complex carbohydrates comprise a greater portion of the carbohydrate content in muntries than in apples. The measured contents of glucose, sucrose, and fructose in apple changed from 10.5%, 28.8%, and 43.3% to 11.3%, 32.1%, and 50.3 % respectively after drying. At the same time, the increase in glucose and fructose content in muntries was from 10.4% to 15.4% and from 16.6% to 22.6% respectively, while sucrose decreased from 17.5% to 10.8%.

Finger limes, too, saw an increase in glucose (1.6% to 2.6%) as well as an increase in fructose (2.4% to 5.0%). Sucrose was not detected in finger limes within the detection limit of the assay. Relative to the initial frozen values, drying had less effect on the glucose, sucrose, and fructose contents of apple compared to the ANFs. The changes to the concentrations of sucrose and fructose in all fruit considered following drying were not substantial enough to be statistically significant. However, drying caused a statistically significant ($p < 0.05$) increase in the glucose content of all fruits. In addition, the effect of drying on glucose content was significantly ($p < 0.05$) greater for both muntries and for finger limes compared to apples. Macronutritional and sugar contents indicate consistency with the previously reported upon tendency for ANFs to be relatively protein-rich compared to conventional fruits, as well as containing lower sugar contents even when higher in carbohydrates overall (Richmond et al., 2019).

Table 4: Changes in sugar contents as a result of oven-drying (at 60°C) of apple, muntrie, and finger lime (per 100 g d.b.). Values attached to different superscripts are statistically significant to each other ($p < 0.05$).

	Apple		Muntrie		Finger Lime	
	Frozen	Dried	Frozen	Dried	Frozen	Dried
Glucose	10.5 ± 1.9^{a1}	11.3 ± 2.3^{a2}	10.4 ± 1.0^{b3}	15.4 ± 0.1^{b4}	1.6 ± 0.4^{c5}	2.6 ± 0.2^{c6}
Sucrose	28.8 ± 8.7^{d}	32.1 ± 3.5^{d}	17.5 ± 1.0^{e}	10.8 ± 2.7^{e}	ND	ND
Fructose	43.3 ± 9.9^{f}	50.3 ± 8.1^{f}	16.6 ± 1.8^{g}	22.6 ± 1.0^{g}	2.4 ± 0.9^{h}	5.0 ± 2.2^{h}

4.7. Comparison of Changes in Sorption to Changes in Carbohydrates

As demonstrated in Section 4.1, the moisture sorption isotherms for ANFs showed the binding of water to the fruit matrix (at temperatures of 40°C and 60°C) was increased after drying. This was contrary to the sorption behaviour of other similar foods, including apples. The extent of this effect depended on drying temperature and drying methods. The processing method that produced the largest effect depended on whether the isotherm was examined above or below an a_w of 0.6-0.8. In simple systems with minimal physical or chemical changes, increases in temperature have the general effect of decreasing sorption due to reduced entropy differences between the adsorbate and unadsorbed material. However, it is not uncommon for food systems to contradict this trend due to physical or chemical temperature-induced material changes (Rao et al., 2005). In particular, the changes in sugar solubility at high water activities (~ 0.8) is known to cause significant deviation. The water activity range above which sugar solubility and crystallinity have significant effects on sugar-rich foods in literature is the same water activity at which the effect of processing on ANF isotherms changed. It is therefore suggested that the uncharacteristic sorption phenomena observed in ANFs are due to drying-induced changes to the sugars present.

546 The changes to the sugar profiles, the cellular features, and the XRD diffractograms that occur as a
547 result of drying support this hypothesis. All samples displaying a reduced amorphous signal after drying
548 suggests the conversion of some portion of the complex carbohydrates present to simpler
549 carbohydrates. Drying was also correlated with the breaking up of organelles and increased area of
550 exposure. Simultaneously, while sucrose and fructose contents are not significantly affected by drying
551 (suggesting inversion is not an explanation), glucose contents are increased significantly, especially in
552 the ANFs. A mechanism for this may be that, during early stages of the drying process when water
553 activity is still high enough for unhindered enzymatic activity, the elevated temperatures of drying
554 allow amylases/glucosidases to convert part of the fruits' starch reserves to glucose. Isomerases may
555 then further partially convert this to fructose. ANFs may see a greater relative increase in these
556 monosaccharides because of a greater activity of these enzymes. This is supported by the fact that the
557 greatest relative increase in fructose and glucose as a result of drying occurred in muntries, suggested
558 by the combination of their macronutritional and sugar profiles to be richer in more complex
559 carbohydrates. It is proposed that this may be a protective mechanism that ANFs have evolved to allow
560 survival in droughts by more substantial access to stored carbohydrate energy in low-moisture
561 circumstances.

562 This effect of drying on carbohydrate chemistry is also reflected in the decrease in monolayer enthalpy
563 as obtained by the fitting of the net isosteric heat of sorption equation (Eq. (6)). The free
564 monosaccharides, with their exposed hydroxyl groups, would present more active sites onto which
565 water can bind, with this solvation layer also being more energetically favourable. Besides supporting
566 the hypothesis described above, the heat of sorption model suggested in this work has the benefit of
567 being a novel and analytical approach to describing sorption phenomena in food systems. Its validity
568 is reinforced by the close agreement with the data reported here. An example of an engineering
569 application is given in Appendix 4. Here the heat required to dry 1 kg each of apples and muntries to
570 a water activity of 0.4 is calculated to be 49 and 92 kJ respectively, reflecting the increased binding
571 energy in muntries. It is proposed that this may be a valuable tool in the design of food dryers for
572 minimal processing by providing the ability to predict energy requirements that can be tuned
573 according to product specifications.

574 5. Conclusions

575 ANFs are crops of significant interest due to their drought tolerance but which lack the characterisation
576 required for larger-scale processing and use, especially when it comes to how they can be most
577 optimally preserved. An understanding of the processing-property relationships and the effects of

processing on shelf-stability of any fruit requires a better understanding of how processing affects the behaviour of the water they contain. This has been addressed in this work by the quantification of water sorption isotherms for finger limes and muntries and subsequent determination of the GAB model as the most suitable descriptor of how they bind moisture. The effects of temperature and processing on these sorption phenomena were measured, showing the unique phenomenon of an increased ability to bind water in muntries and finger limes following drying. XRD and TEM revealed an opening up of cellular features and a reduction in the amount of amorphous complex carbohydrates during drying. Macronutritional and sugar characterisation demonstrated high protein contents as well as a significant drying-induced increase in glucose content. The increase in water binding after drying in ANFs is suggested to be the result of more substantial hydrolysis of complex polysaccharides during drying. The temperature variation of the isotherms was also used to determine the net isosteric heat of sorption as a function of moisture content, with a precision that allowed the derivation of a novel analytical expression for this function. Applications of this expression include the calculation of the heat required to dry the fruits studied to a target water activity. These results provide tools for the engineering of drying processes to extend ANF shelf-life as much as needed while drying as little as possible for the water activity needed. This allows for reduced energy use in drying and minimal quality losses. The models and techniques developed in this paper allow this not only for ANFs but for the more sustainable processing of foods more generally.

Acknowledgments

The authors wish to acknowledge the traditional custodians of the land where the work of this project took place, the Bunurong people of the Kulin Nation, as well as the traditional custodians of the Wotjobaluk, Jaadwa, Jadawadjali, Wergaia and Jupagulk people on whose lands the foods that were studied were grown. The authors wish to pay respects to their Elders, past and present and to their continual connection to the lands.

The authors especially wish to thank the traditional growers who shared their knowledge to aid this project, in particular Elizabeth Mace a Wotjobaluk, Jadawadjali and Wergaia Woman from the Barengi Gadjin Land Council.

Special thanks also go to Ni Ni Well and OZ Finger Lime for their insights and samples.

Declaration of interest statement

The authors declare that they have no known competing financial interests or personal relationships that could have appeared to influence the work reported in this paper.

References

AL-MUHTASEB, A. H., MCMINN, W. A. M. & MAGEE, T. R. A. 2002. Moisture Sorption Isotherm Characteristics of Food Products: A Review. *Food and Bioproducts Processing,* 80**,** 118-128.

AOAC, J. 2005. *Official Methods of Analysis of AOAC International,* Gaithersburg, MD, USA.

BEN HAJ SAID, L., BELLAGHA, S. & ALLAF, K. 2015. Measurements of texture, sorption isotherms and drying/rehydration kinetics of dehydrofrozen-textured apple. *Journal of Food Engineering,* 165**,** 22-33.

BEZERRA, R., SILVA, M., MORAIS, I., OSAJIMA, J., SANTOS, M., AIROLDI, C. & FILHO, E. 2014. Phosphated Cellulose as an Efficient Biomaterial for Aqueous Drug Ranitidine Removal. *Materials,* 7**,** 7907-7924.

BURNS, J., ACHOR, D. & ECHEVERRIA, E. 1992. Ultrastructural Studies on the Ontogeny of Grapefruit Juice Vesicles (Citrus paradisi Macf. CV Star Ruby). *International Journal of Plant Sciences - INT J PLANT SCI,* 153.

CHUNG, D. S. & PFOST, H. B. 1967. Adsorption and Desorption of Water Vapor by Cereal Grains and Their Products Part I: Heat and Free Energy Changes of Adsorption and Desorption. *Transactions of the ASABE,* 10**,** 549-0551.

ESCOBEDO-AVELLANEDA, Z., VELAZQUEZ, G., TORRES, J. A. & WELTI-CHANES, J. 2012. Inclusion of the variability of model parameters on shelf-life estimations for low and intermediate moisture vegetables. *LWT,* 47**,** 364-370.

FRANCINI, A. & SEBASTIANI, L. 2013. Phenolic Compounds in Apple (Malus x domestica Borkh.): Compounds Characterization and Stability during Postharvest and after Processing.

GLOVER, R., TAYLOR, T., REDMAN, M. & TRAINER, P. 2021. Australian Native Finger Lime RD&E Plan. AgriFutures.

HOSSAIN, M. D., BALA, B. K., HOSSAIN, M. A. & MONDOL, M. R. A. 2001. Sorption isotherms and heat of sorption of pineapple. *Journal of Food Engineering,* 48**,** 103-107.

IGLESIAS, H. A. & CHIRIFE, J. 1978. An Empirical Equation for Fitting Water Sorption Isotherms of Fruits and Related Products. *Canadian Institute of Food Science and Technology Journal,* 11**,** 12-15.

JEANTET, R. 2016. *Handbook of food science and technology. 1, Food alteration and food quality,* London : Hoboken, London : ISTE, Ltd. Hoboken : Wiley.

KAYMAK-ERTEKIN, F. & GEDIK, A. 2004. Sorption isotherms and isosteric heat of sorption for grapes, apricots, apples and potatoes. *Food science & technology,* 37**,** 429-438.

KAZEMI, M., ABOUTALEBZADEH, S., MOJAVERIAN, S. P., SAMANI, S. A., KOUHSARI, F., POURVATANDOUST, S., SALIMI, A., SAVAROLYIA, M., NAJAFI, A., HOSSEINI, S. S. & KHODAIYAN, F. 2023. Valorization of pistachio industrial waste: Simultaneous recovery of pectin and phenolics, and their application in low-phenylalanine cookies for phenylketonuria. *International Journal of Biological Macromolecules,* 249**,** 126086.

KIRANOUDIS, C. T., MAROULIS, Z. B., TSAMI, E. & MARINOS-KOURIS, D. 1993. Equilibrium moisture content and heat of desorption of some vegetables. *Journal of Food Engineering,* 20**,** 55-74.

LAURIE, S. 2020. Australian native foods and botanicals- 2019/20 market study. ANFAB.

MAROULIS, Z. B., TSAMI, E., MARINOS-KOURIS, D. & SARAVACOS, G. D. 1988. Application of the GAB model to the moisture sorption isotherms for dried fruits. *Journal of food engineering,* 7**,** 63-78.

MERRILL, A. L. 1973. Energy Value of Foods: Basis and Derivation. *In:* AGRICULTURE, U. S. D. O. (ed.).

MORAGA, G., MARTÍNEZ-NAVARRETE, N. & CHIRALT, A. 2006. Water sorption isotherms and phase transitions in kiwifruit. *Journal of Food Engineering,* 72**,** 147-156.

MORAGA, G., TALENS, P., MORAGA, M. J. & MARTÍNEZ-NAVARRETE, N. 2011. Implication of water activity and glass transition on the mechanical and optical properties of freeze-dried apple and banana slices. *Journal of Food Engineering,* 106**,** 212-219.

MOREIRA, R., CHENLO, F., TORRES, M. D. & VALLEJO, N. 2008. Thermodynamic analysis of experimental sorption isotherms of loquat and quince fruits. *Journal of Food Engineering,* 88**,** 514-521.

MUTUNGI, C., PASSAUER, L., ONYANGO, C., JAROS, D. & ROHM, H. 2012. Debranched cassava starch crystallinity determination by Raman spectroscopy: Correlation of features in Raman spectra with X-ray diffraction and 13C CP/MAS NMR spectroscopy. *Carbohydrate Polymers,* 87**,** 598-606.

NETZEL, M., NETZEL, G., TIAN, Q., SCHWARTZ, S. & KONCZAK, I. 2007. Native Australian fruits — a novel source of antioxidants for food. *Innovative Food Science & Emerging Technologies,* 8**,** 339-346.

O'BRIEN, S. & WANG, Y.-J. 2008. Susceptibility of annealed starches to hydrolysis by α-amylase and glucoamylase. *Carbohydrate Polymers,* 72**,** 597-607.

ORIANS, G. H. & MILEWSKI, A. V. 2007. Ecology of Australia: the effects of nutrient-poor soils and intense fires.

RAO, M. A., RIZVI, S. S. H. & DATTA, A. K. 2005. *Engineering properties of foods,* Boca Raton, Taylor & Francis.

RICHMOND, R., BOWYER, M. & VUONG, Q. 2019. Australian native fruits: Potential uses as functional food ingredients. *Journal of Functional Foods,* 62**,** 103547.

SALO-VÄÄNÄNEN, P. P. & KOIVISTOINEN, P. E. 1996. Determination of protein in foods: comparison of net protein and crude protein (N × 6.25) values. *Food Chemistry,* 57**,** 27-31.

SENEVIRATNE, S. I., ZHANG, X., ADNAN, M. & W. BADI; C. DERECZYNSKI, A. D. L., S. GHOSH, I. ISKANDAR, J. KOSSIN, S., LEWIS, F. OTTO, I. PINTO, M. SATOH, S.M. VICENTE-SERRANO, M. WEHNER, B. ZHOU 2023. Weather and Climate Extreme Events in a Changing Climate. *In:* INTERGOVERNMENTAL PANEL ON CLIMATE, C. (ed.) *Climate Change 2021 – The Physical Science Basis: Working Group I Contribution to the Sixth Assessment Report of the Intergovernmental Panel on Climate Change.* Cambridge: Cambridge University Press.

TSAMI, E. 1991. Net isosteric heat of sorption in dried fruits. *Journal of Food Engineering,* 14**,** 327-335.

TSAMI, E., KROKIDA, M. K. & DROUZAS, A. E. 1998. Effect of drying method on the sorption characteristics of model fruit powders. *Journal of Food Engineering,* 38**,** 381-392.

TSAMI, E., MAROULIS, Z. B., MARINOS-KOURIS, D. & SARAVACOS, G. D. 1990. Heat of sorption of water in dried fruits. *International Journal of Food Science & Technology,* 25**,** 350-359.

USDA 2018. Apples, raw, with skin (Includes foods for USDA's Food Distribution Program).

VAN 'T HAG, L., DANTHE, J., HANDSCHIN, S., MUTULI, G., MBUGE, D. & MEZZENGA, R. 2020. Drying of African Leafy Vegetables for Their Effective Preservation: Difference in Moisture Sorption Isotherms Explained by their Microstructure. *Food & Function,* 11.

YE, S.-J. & BAIK, M.-Y. 2024. Physicochemical properties of amorphous granular starch (AGS) prepared by non-thermal gelatinization by high hydrostatic pressure (HHP) and spray drying. *International Journal of Biological Macromolecules,* 260**,** 129508.

ZHANG, A.-A., XIE, L., WANG, Q.-H., XU, M.-Q., PAN, Y., ZHENG, Z.-A., LV, W.-Q. & XIAO, H.-W. 2024. Effect of the ripening stage on the pulsed vacuum drying behavior of goji berry (Lycium barbarum L.): Ultrastructure, drying characteristics, and browning mechanism. *Food Chemistry,* 442**,** 138489.